Title
Geometry and electronic structure of iridium adsorbed on graphene

Journal
Physical Review B, 99(7)

ISSN
2469-9950

Authors
Barker, BA
Bradley, AJ
Ugeda, MM
et al.

Publication Date
2019-02-22

DOI
10.1103/PhysRevB.99.075431

Peer reviewed

The Geometry and Electronic Structure of Iridium adsorbed on Graphene

Bradford A. Barker, [1, 2, *] Aaron J. Bradley, [1, 2] Miguel Moreno Ugeda, [3, 4] Sinisa Coh, [5]

Alex Zettl, [1, 2] Michael F. Crommie, [1, 2] Steven G. Louie, [1, 2] and Marvin L. Cohen [1, 2]

1) Department of Physics, University of California, Berkeley, CA 94720, USA

2) Materials Sciences Division, Lawrence Berkeley National Laboratory, Berkeley, CA 94720, USA

3) Ikerbasque, Basque Foundation for Science, 48013 Bilbao, Spain

4) CIC nanoGUNE, 20018 San Sebastián, Spain

5) Department of Mechanical Engineering, University of California, Riverside, CA 92521, USA

*) bbarker@civet.berkeley.edu

ABSTRACT

The geometry and electronic structure of Iridium atoms adsorbed on graphene are investigated through a combined experimental and theoretical study. Ir atoms are deposited on a flake of graphene on a Pt(111) surface, where it is found that Ir atoms tend to form clusters, even at low temperatures. The areal density of the observed clusters on the graphene flake suggests the clusters are most likely to be a pair of

Ir atoms. Theoretical ab initio density functional (“DFT”) calculations indicate that these Ir dimers are oriented horizontally, near neighboring “bridge” sites of the graphene lattice, as this configuration has the strongest adsorption energy of all high-symmetry configurations for the Ir dimer. A large peak in the LDOS at the Dirac point energy is measured via scanning tunneling spectroscopy, and this result is reproduced by a DFT calculation of the local density of states (“LDOS”). This peak at the Dirac point energy is found to be from the Ir s and p states. The LDOS in the monomer case is also calculated, and it is found to be significantly different than the experimentally determined result.

I. INTRODUCTION

The sublattice symmetry of graphene results in a Dirac-like low-energy Hamiltonian about the K and K’ points in its Brillouin Zone, which gives it the remark able electronic properties of ultrarelativistic chiral Dirac fermions, such as ballistic transport and the anomalous Integer Quantum Hall Effect [1] . Much experimental and theoretical work has been devoted to the manipulation of graphene to modify its electronic structure in novel ways.

A subset of these works focuses on investigating how adatoms and other adsorbates modify various electronic properties of graphene. The electronic structure of graphene with a dozen different adatoms was calculated in Ref. 2, finding slight modifications to the electronic density of states (DOS) with alkali adatoms and considerable modification to the DOS with transition metal adatoms. In particular, the linear DOS in the vicinity of the Dirac point was largely obscured

by the d-like atomic states from transition metal adatoms Ti, Fe, and Pd, and the noble metal adatom Au [2] .

Theoretical studies of Pd dimers adsorbed onto graphene have shown potential for hydrogen storage, as well. Pairs of hydrogen atoms prefer to dissociate and bond on opposing sides of Pd dimers instead of forming a hydrogen bond [3] . Similar results have also been reported for larger Pd clusters [4] .

Further theoretical work [5–10] has focused on enhancing the weak spin-orbit coupling of graphene by using adatoms to break symmetries, as well as the intrinsic contribution of the atomic spin-orbit coupling from sufficiently heavy metallic adatoms. In particular, calculations with Au [6] , W [7] , Os [11] , Ir [11] , and In [12] adatoms suggested relatively large spin-orbit gaps with non-trivial band topologies.

Attempts at realizing these exotic electronic phases with In adatoms [13] and W adatoms [14] have shown null results, however. Initial theoretical work suggested that the adsorption of In onto the hollow site of graphene allows for a fortuitous cancellation of the Rashba spin orbit coupling [12] , thus allowing an induced quantum spin Hall effect. However, enhancement of the Coulomb scattering from the defect rendered any possible non-trivial topology unobservable. Refined first-principles scattering calculations using the quasiparticle band structure with spin-orbit coupling treated non-perturbatively [14] have supported this interpretation.

Additionally, the work with Os and Ir adatoms noted that monomers form spin moments of 0.45 μ_B and 0.30 μ_B per atom, respectively [11] , breaking the time-reversal invariance required for the quantum spin Hall effect. Dimerizing the

transition metal atoms with Cu was proposed to eliminate magnetic moments in the system and thus preserve time-reversal symmetry [11] .

In a combined experimental and theoretical study, the Ir atoms are shown to form dimers on graphene, with the electronic structure of the dimers featuring a large contribution to the local density of states (“LDOS”) at the Dirac point energy. Section II presents the experimental work of using vapor deposition to adsorb Ir atoms onto graphene and then using scanning tunneling miscroscopy (“STS”) measurements to analyze the electronic features. In Section IV, density functional calculations to further understand the geometry of the adsorbed Ir atoms as well as their electronic structure are presented. The theoretical results indicate that the Ir dimer adsorbates bind in a horizontal configuration along the carbon-carbon bond sites, in contrast with the prediction of vertical dimers binding to the hollow site in a ring of carbon atoms 11 . In Section V, the results of calculations of the LDOS are shown to suggest that the 6s and 6p states from the Ir atoms contribute to the peak in the LDOS at the Dirac point energy. The calculated peak in the LDOS is shown to have good agreement with the measured spectra.

II. EXPERIMENTAL RESULTS

All STM and STS measurements were carried out at T = 7K in an ultra-high vacuum (UHV) environment using a homebuilt scanning tunneling microscope. Graphene was grown on Pt(111), and Ir was deposited on cold samples using an Omicron e-beam evaporator. The maximum temperature of the sample during Ir evaporations ranged between 8K and 12K, with different temperatures leading to qualitatively similar coverages.

Fig. 2a shows a typical STM image of Ir clusters on bare Pt(111) and graphene/Pt(111). The voltage is set to +0.33 V, with the tunneling current 1 nA. The graphene patch is outlined with a dotted green line. The Ir clusters appear as orange protrusions, with the clusters on the graphene patch appearing significantly larger than those on the bare Pt(111) surface. The identical protrusions observed on Pt(111) are identified as single Ir adatoms due to the absence of thermally-driven Ir diffusion on Pt(111) at such a low temperatures [15] . Unlike on Pt(111), the size of the clusters on the graphene surface is not homogeneous, likely indicating a varying number of atoms per cluster.

STS curves from three different Ir clusters on graphene are shown in Fig. 2b. For each of these clusters, there is a feature in the spectra that occurs at around +0.33 V, which is similar in energy to the Dirac point of graphene on Pt(111) [16,17] , as well as the onset of an unoccupied Pt(111) surface state [18] . The STS curves also exhibit a feature at higher energy, centered at +1.2 V. The lock-in parameters are f = 2140 Hz, I t = 1 nA, V rms = 4 mV.

A conductance map taken at V bias = +0.33 V, the energy of the large STS feature, is shown in Fig. 2c. As can be seen, a number of clusters exhibit the spectral feature at +0.33 V. The lock-in parameters are the same as before, except with V rms = 5 mV.

To better understand the distribution of clusters on the surface, the atom density may be estimated from a plot of the number of clusters as a function of the area of a graphene island for a given set of evaporation parameters, as shown in Fig. 2d. The black dashed line is the expected number of clusters if all were indeed single Ir atoms, equal to the density of Ir atoms on the bare Pt(111)

surface. The red dashed line is the expected number of clusters if all were dimers. The majority of our data points fall closer to the dimer line, suggesting that Ir adatoms are mobile on graphene at temperatures as low as 8K and cluster with a small number of atoms, likely forming dimers and, less frequently, trimers. The mobility of Ir adatoms on graphene may also be affected by the superlattice formed between graphene and the Pt(111).

III. CALCULATION METHODS

The ab initio calculations [19] of the system are performed using the Quantum ESPRESSO [20] density functional theory software package. A 4×4 supercell is used for the single adatom and vertically-oriented dimer systems, and a 5x5 supercell is used for the horizontally-oriented dimer, with a vacuum of 15 Å in all cases, as measured from the topmost Ir atom in the system. The psuedopotentials are Vanderbilt ultrasoft fully relativistic pseudopotentials [21,22] , along with a 40 Ry planewave kinetic energy cutoff and a 381 Ry charge density planewave cutoff. The LDA is chosen for the exchange-correlation functional in the pseudopotentials, which in the context of graphene adsorbed on a Ir(111) surface gives similar results as compared with van der Waals functionals [23] , and is the choice consistent with Ref. 11. The metallic bonding of Ir to graphene is adequately described in the LDA, despite the systematic overestimation of binding. The Methfessel-Paxton smearing [24] , appropriate for metals, has a width 0.005 Ry. The Monkhorst-Pack grid for sampling the Brillouin zone was 9×9×1 when constructing the charge density. The computational details for the DOS calculations are in Section V.

The computed carbon-carbon distance of 1.417 Å agrees well with the experimental value of 1.42 Å, found by relaxing the primitive unit cell for graphene. The binding energy of a single adatom is calculated from $\Delta E = E_{tot} - E_{gr} - E_{Ir}$, where E_{tot} is the energy of the Ir adatom-on-graphene system, E_{gr} is the energy of an isolated graphene supercell, and E_{Ir} is the energy of an isolated Ir atom. For the adsorbed dimer systems, the binding energy per Ir atom is defined as $\Delta E = 1/2\ (E_{tot} - E_{gr} - 2E_{Ir})$, with E_{tot} now referring to the Ir dimer-on-graphene system. The value of E_{gr} is scaled appropriately for the size of the supercell under consideration.

The Pt(111) substrate is not explicitly included in the calculations. The graphene-Pt substrate interaction will not by itself introduce a gap in the graphene Dirac cone [25], with the substrate merely introducing hybridization effects that obscure the usual linear dispersion. The dominant physical effect of the substrate is considered implicitly by fixing the positions of the carbon atoms in the graphene sheet. The carbon atoms are held fixed when determining the relaxed coordinates of the Ir atoms. In comparing the results of the theoretical calculations to experiment, the particular values of Fermi energy differ due to the neglect of the Pt substrate, so the theoretical and experimental spectra are instead compared near the estimated Dirac point energy, E_D. This energy E_D is taken to be the zero of energy for all theoretical calculations.

Hopping matrix elements between Ir atoms in neighboring supercells, computed in Wannier90 [26], were found to be at most 2 meV, indicating that the wavefunctions are well-contained in a single supercell. The small in-3 tercellular interaction was confirmed by a 6×6 supercell calculation for the $H^1 - H^2$

system, as the adsorption energy per Ir atom changes by only 7 meV, relative to the 5×5 supercell.

IV .THEORETICAL GEOMETRY

A. Single adatom

The Ir adatom is relaxed in the bridge (“B”), hollow (“H”), and top (“T ”) sites (shown in Fig. 1). The Ir atom favors the B site, in agreement with previous calculations using PBE and van der Waals functionals [27] , in addition to calculations of single-adatom Pd [2] . Ref. 11 finds a preference for the H site using LDA while neglecting to include corrections to the dipole interaction with periodic images in the out-of-plane direction. This result is reproduced when performing the single-atom relaxation while neglecting the correction to the dipole interaction.

Table I summarizes the binding heights h, adsorption energies ΔE, diffusion barries E_{Diff} , and magnetic moment per supercell m, and effective charge Q for the single Ir adsorption. The estimate of the effective charge indicates a donation of electrons from Ir to the graphene sheet, while the magnetic moment per supercell of nearly 1 μ_B is consistent with an effective charge of 4.88e, indicating an uncompensated additional spin at the Ir atom.

The diffusion barrier across a high-symmetry point is approximated as $E_{Diff} = E_{a\,max} - \Delta E$, the difference in energy from the lowest-energy geometry to the energy of the site under consideration [2] . The most appropriate approximation of the diffusion path would be one that is calculated by the nudged elastic band method to explore the full energy surface for all possible directions. However, if the diffusion is assumed most likely to occur nearly along high-symmetry

directions, the barrier to diffusion along a direction is simply the difference in energy of the initial and final configurations. The estimated diffusion barriers of 0.73 eV and 0.49 eV for the top and hollow sites, respectively, are well-above room temperature and are on the order of that of Fe adsorbed on graphene [2].

The tendency for the adatoms on graphene to form clusters can be estimated by comparing the binding energy per atom ΔE to the bulk cohesive energy per atom E_c. A ratio of $\Delta E/E_c \sim 1$ indicates a strong adsorption energy of the adatom and therefore a tendency to bind to graphene as an adatom; the opposite limit indicates a tendency to cluster. However, the LDA overestimates cohesive energies for solids, particularly 5d transition metals [28], so instead the experimental value of $E_c = 6.94$ eV [28] is used. With the adsorption energy at the bridge site $\Delta E = 1.86$ eV, the ratio is 0.268. Though this ratio may still be overestimated due to the use of the LDA for the calculation of the binding energy, this result may be compared to the value of 0.307 reported for Al$_2$, which is also known experimentally to form clusters with three atoms when adsorbed to graphite [29,30]. Based on this, the estimation suggests that Ir tends to cluster on graphene, which is supported by experiment (Fig. 2d).

B. Dimer

The horizontal dimer at the bridge sites B^1 and B^2 (see Fig. 1) has the largest adsorption energy for any of the considered dimer configurations, horizontal or vertical, so it is the most likely orientation for the observed two-atom clusters at low temperature. The bonding distances for the horizontal dimers (2.32-2.46 Å) are longer than in isolation, 2.23 Å [31], and are on the order of the C-C bond length, 2.46 Å. Indeed, the bridge-site dimer has the shortest Ir-Ir distance,

explaining its favorable adsorption energy, as it is stretched from its value in isolation the least. By comparing the adsorption energy per atom for this dimer (Table II) and the single adatom (Table I), it is found that each Ir atom favors the formation of a dimer by 1.5 eV.

The estimated diffusion barrier is computed for the dimer as a whole, defined from $E_{Diff} = 2\,(E_{a\,max} - \Delta E)$. The hollow site has an estimated diffusion barrier of 1.02 eV, indicating a stronger preference to diffuse through the top site, with much lower estimated diffusion barrier of 0.34 eV, which may allow a pathway to form larger clusters. The estimated charge per Ir atom, 4.99e, is slightly larger than its single-adatom value, 4.88e, indicating that less charge is transferred to the graphene sheet due to the presence of the dimer bond. The magnetic moment per unit-cell is consequently increased to over 1 μ_B per Ir atom. The magnetic moment now has a large in-plane component in addition to the out-of-plane component, due to the in-plane dimer bond defining an additional axis for the magnetic moment.

The binding energies per Ir atom in the vertical configuration are nearly identical for the B, H, and T positions, with 3.11 eV for B and T , and 3.14 eV for H, giving small diffusion barriers of 0.06 eV, comparable to room temperature. The dimer bond lengths are nearly the same as the isolated dimer bonding length of 2.17 Å. The distances from the bottom-most Ir atom in the dimer from the graphene sheet (h_b in Table III) are larger than the single Ir adatom case.

V. ELECTRONIC STRUCTURE

A. Single adatom

The DOS of pristine graphene in a primitive unit cell is calculated with a 96×96×1 Monkhorst-Pack grid, which is dense enough to resolve the zero DOS at the Dirac point energy. An adsorbate atop a 4×4 supercell of graphene needs only a 24×24×1 grid to give an overall sampling density equivalent to that of pristine graphene[4] for DOS calculations. The peaks in the DOS from the weakly-hybridized, low-lying sp^2 states may be matched with that of pristine graphene (Fig. 3) to provide an estimate to the Dirac point.

For comparison with the experimental STS spectra, the LDOS is calculated by integrating the density of states 4 Å above the Ir atoms. The delta functions in the LDOS are taken to be Gaussian functions with a smearing of 75 meV. The actual tip to atom distance is estimated to be 5 to 10 Å.

The LDOS (Fig. 4) shows a significant peak placed about 1 eV above the Dirac point energy, with a much weaker peak at the Dirac point energy. This indicates that the experimentally observed peaks (Fig. 2c) do not come from this configuration of single adatoms. By comparing the LDOS with the partial density of states resolving the s, p, and d Ir states (Fig. 5), the Ir s- and p-states are found to give the most significant contribution to the large peak, with the d-states being localized below the 4 Å simulated tip placement.

B. Dimer

The DOS, LDOS, and PDOS for the adsorbed dimer system are similarly computed. Again, the DOS (Fig. 6) shows that the low-lying sp^2 states from graphene are only weakly hybridized with the Ir states and therefore allow for an estimation of the Dirac point energy.

The LDOS places a large peak near the estimated Dirac point energy (Fig. 7), as observed in experiment. This suggests that the Ir clusters are indeed a pair of B-site Ir adatoms in the horizontal configuration. The PDOS (Fig. 8) shows a significant contribution from the Ir 5d states. However, comparing the LDOS with the PDOS (Fig. 9), the features of the LDOS, especially within a 1 eV window about the Dirac point energy, appear to arise from the sum of the 6s- and 6p-states, as these states have a longer spatial extent than the 5d states.

Fig. 10 directly compares the measured dI/dV spectrum with the calculated LDOS, plotted in arbitrary units such that both curves are matched at the central peak height. There is good agreement with the placement of the central peak, with the few meV difference resulting from any accumulated systematic errors in both the experimental and theoretical estimations for its placement. The higher-energy feature also seems to be reproduced, though within a significantly red-shifted energy range, likely due to DFT underestimating such excited-state features. The peaks below the estimated Dirac point energy that are present in the calculated LDOS are suppressed in the measured spectrum. Otherwise, the agreement between experiment and theory is satisfactory.

VI. CONCLUSION

Ir atoms deposited on graphene on Pt(111) are found to form clusters, even at low temperatures. By calculating the areal density of the observed clusters on the graphene flake, the typical size of the clusters are estimated to be composed of two Ir atoms. Through ab initio density functional calculations, the Ir dimer is found to be oriented horizontally, at the bridge sites of the graphene lattice. The peaks in the experimental and theoretical LDOS near the estimated Dirac point

energy match well and may be attributed to the Ir dimer 6s and 6p states. The LDOS for a single adatom is found to have significantly different peak locations and amplitudes than that of experiment.

VII. ACKNOWLEDGMENTS

The authors would like to thank Sehoon Oh and Ting Cao for useful discussions. [Not sure about this grant number???] This work was supported by National Science Foundation Grant No. DMR-1508412 and by the Director, Office of Science, Office of Basic Energy Sciences, Materials Sciences and Engineering Division, U.S. Department of Energy under Contract No. DE-AC02-05CH11231. Computational resources have been provided by the DOE at Lawrence Berkeley National Laboratory's NERSC facility.

REFERENCES

[1] A. H. Castro Neto, F. Guinea, N. M. R. Peres, K. S. Novoselov, and A. K. Geim, Rev. Mod. Phys. 81, 109 (2009).

[2] K. T. Chan, J. B. Neaton, and M. L. Cohen, Phys. Rev. B 77, 235430 (2008).

[3] I. Lopez-Corral, E. Germán, A. Juan, M. Volpe, and G. Brizuela, international journal of hydrogen energy 37, 6653 (2012).

[4] I. Cabria, M. López, S. Fraile, and J. Alonso, The Journal of Physical Chemistry C 116, 21179 (2012).

[5] A. H. Castro Neto and F. Guinea, Phys. Rev. Lett. 103, 026804 (2009).

[6] D. Ma, Z. Li, and Z. Yang, Carbon 50, 297 (2012).

[7] H. Zhang, C. Lazo, S. Blügel, S. Heinze, and Y. Mokrousov, Phys. Rev. Lett. 108, 056802 (2012).

[8] Y. Li, P. Tang, P. Chen, J. Wu, B.-L. Gu, Y. Fang, S. B. Zhang, and W. Duan, Phys. Rev. B 87, 245127 (2013).

[9] J. Ding, Z. Qiao, W. Feng, Y. Yao, and Q. Niu, Phys. Rev. B 84, 195444 (2011).

[10] Z. Qiao, S. A. Yang, W. Feng, W.-K. Tse, J. Ding, Y. Yao, J. Wang, and Q. Niu, Phys. Rev. B 82, 161414 (2010).

[11] J. Hu, J. Alicea, R. Wu, and M. Franz, Phys. Rev. Lett. 109, 266801 (2012).

[12] C. Weeks, J. Hu, J. Alicea, M. Franz, and R. Wu, Phys. Rev. X 1, 021001 (2011).

[13] Z. Jia, B. Yan, J. Niu, Q. Han, R. Zhu, D. Yu, and X. Wu, Phys. Rev. B 91, 085411 (2015).

[14] F. J. d. Santos, D. A. Bahamon, R. B. Muniz, K. McKenna, E. V. Castro, J. Lischner, and A. Ferreira, arXiv:1712.07827 (2017).

[15] D. Bassett and P. Webber, Surface Science 70, 520 (1978).

[16] P. Sutter, J. T. Sadowski, and E. Sutter, Phys. Rev. B 80, 245411 (2009).

[17] M. M. Ugeda, D. Fernández-Torre, I. Brihuega, P. Pou, A. J. Martínez-Galera, R. Pérez, and J. M. Gómez-Rodríguez, Phys. Rev. Lett. 107, 116803 (2011).

[18] J. Wiebe, F. Meier, K. Hashimoto, G. Bihlmayer, S. Blügel, P. Ferriani, S. Heinze, and R. Wiesendanger, Phys. Rev. B 72, 193406 (2005).

[19] M. L. Cohen, M. Schlüter, J. R. Chelikowsky, and S. G. Louie, Phys. Rev. B 12, 5575 (1975).

[20] P. Giannozzi, S. Baroni, N. Bonini, M. Calandra, R. Car, C. Cavazzoni, D. Ceresoli, G. L. Chiarotti, M. Cococcioni, I. Dabo, A. D. Corso, S. de Gironcoli, S. Fabris, G. Fratesi, R. Gebauer, U. Gerstmann, C. Gougoussis, A. Kokalj, M. Lazzeri, L. Martin-Samos, N. Marzari, F. Mauri, R. Mazzarello, S. Paolini, A. Pasquarello, L. Paulatto, C.

Sbraccia, S. Scandolo, G. Sclauzero, A. P. Seitsonen, A. Smogunov, P. Umari, and R. M. Wentzcovitch, Journal of Physics: Condensed Matter 21, 395502 (2009).

[21] D. Vanderbilt, Phys. Rev. B 41, 7892 (1990).

[22] A. Dal Corso, Computational Materials Science 95, 337 (2014).

[23] R. Brako, D. Šokčević, P. Lazić, and N. Atodiresei, New Journal of Physics 12, 113016 (2010).

[24] M. Methfessel and A. T. Paxton, Phys. Rev. B 40, 3616 (1989).

[25] Q. Zhou, S. Coh, M. L. Cohen, S. G. Louie, and A. Zettl, Phys. Rev. B 88, 235431 (2013).

[26] A. A. Mostofi, J. R. Yates, Y.-S. Lee, I. Souza, D. Vanderbilt, and N. Marzari, Computer Physics Communications 178, 685 (2008).

[27] I. A. Pašti, A. Jovanović, A. S. Dobrota, S. V. Mentus, B. Johansson, and N. V. Skorodumova, arXiv:1710.08985 (2017).

[28] R. E. Watson, G. W. Fernando, M. Weinert, Y. J. Wang, and J. W. Davenport, Phys. Rev. B 43, 1455 (1991).

[29] E. Ganz, K. Sattler, and J. Clarke, Surface Science 219, 33 (1989).

[30] V. Maurice and P. Marcus, Surface Science 275, 65 (1992).

[31] J. L. Jules and J. R. Lombardi, The Journal of Physical Chemistry A 107, 1268 (2003).

TABLE I: For the hollow, bridge, and top configurations, the heights h, the binding energy ΔE of the single Ir atom adsorbed to graphene in the LDA, the diffusion

barrier, the magnetic moment per supercell, and the estimation of the local charge of the Ir atom are calculated.

Config.	h (Å)	ΔE (eV)	(eV)	m (μ_B)	Q (e)
Bridge	1.95	1.86	–	0.95	4.88
Hollow	1.70	1.13	0.73	0.61	5.32
Top	1.93	1.37	0.49	0.99	4.55

TABLE II: For the hollow, bridge, and top configurations in which the Ir atoms are placed at the B/H/T 1 and B/H/T 2 sites, the calculated relaxed z-coordinates of each Ir atom, the adsorption energy ΔE of the horizontally-oriented Ir dimer adsorbed to graphene in the LDA, the estimate of the diffusion energy, the cartesian components of the magnetic moment per supercell, and the local charge for each Ir atom are presented.

Config.	h(Å)	$d_{Ir\text{-}Ir}$ (Å)	ΔE (eV)	E_{diff} (eV)	m_x (μ_B)	m_y (μ_B)	m_z (μ_B)	Q (e)
B^1-B^2	2.05	2.32	3.36	–	0.00	1.06	1.29	4.99
H^1-H^2	1.88	2.46	2.85	1.02	0.00	0.00	1.32	5.68
T^1-T^2	2.10	2.45	3.19	0.34	0.23	0.23	1.28	5.04

TABLE III: For the vertically-oriented dimer in the hollow, bridge, and top configurations, the calculated relaxed z-coordinates, the adsorption energy ΔE of the vertically-oriented Ir dimer adsorbed to graphene in the LDA, the estimate of the diffusion energy, the (out-of-plane) magnetic moments for each Ir atom, the total magnetic moment per supercell, and the local charge for each Ir atom are presented. The lowest energy for all dimers is found in the horizontal $B^1 - B^2$ configuration.

Config.	h_b (Å)	$d_{Ir\text{-}Ir}$ (Å)	ΔE (eV)	E_{diff} (eV)	m_b (μ_B)	m_t (μ_B)	m (μ_B)	Q (e)	Q (e)
Bridge	2.41	2.19	3.11	0.06	0.58	0.67	2.07	5.08	5.11
Hollow	2.29	2.19	3.14	–	0.54	0.77	2.00	5.03	5.13
Top	2.40	2.18	3.11	0.06	0.58	0.68	2.05	5.05	5.08

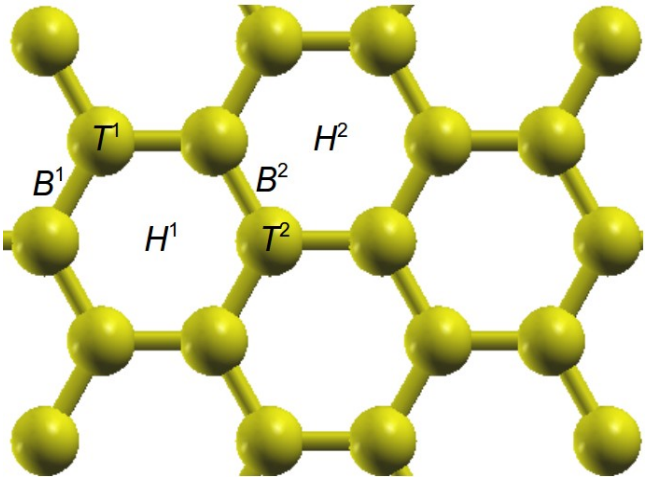

FIG. 1: The adsorption sites considered: bridge (B^1 ,B^2), hollow (H^1 , H^2), and top (T^1 , T^2). In the monomer and vertical dimer cases, only B^1 , H^1 , and T^1 are considered and are referred to as B, H, and T , respectively.

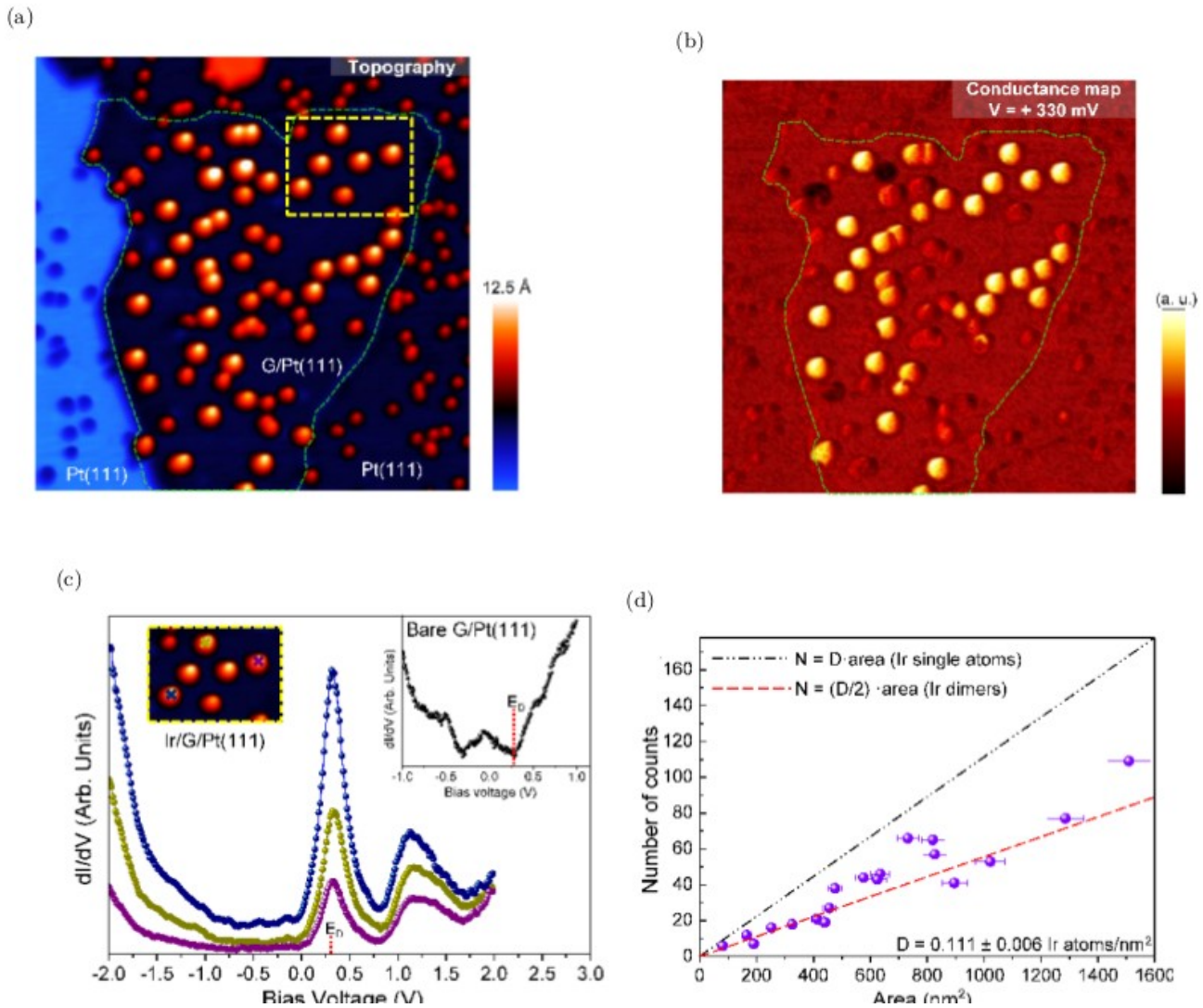

FIG. 2: (2a): The STM topography of Ir clusters on bare Pt(111) and graphene on Pt(111). The graphene flake is within the green dotted contour, and the Ir clusters under consideration are within the yellow dotted rectangle. (2b): The conductance map of the same region. (2c): The conductance maps for the indicated Ir clusters in the top-left inset. The top-right inset is the spectrum for the graphene flake away from the Ir clusters. The estimated Dirac point is indicated by the vertical dashed red line. (2d): The number of clusters as a function of the area of the

graphene island. The dash-dotted black line has a slope with a density for that of one Ir atom per cluster, and the dashed red line, two Ir atoms per cluster.

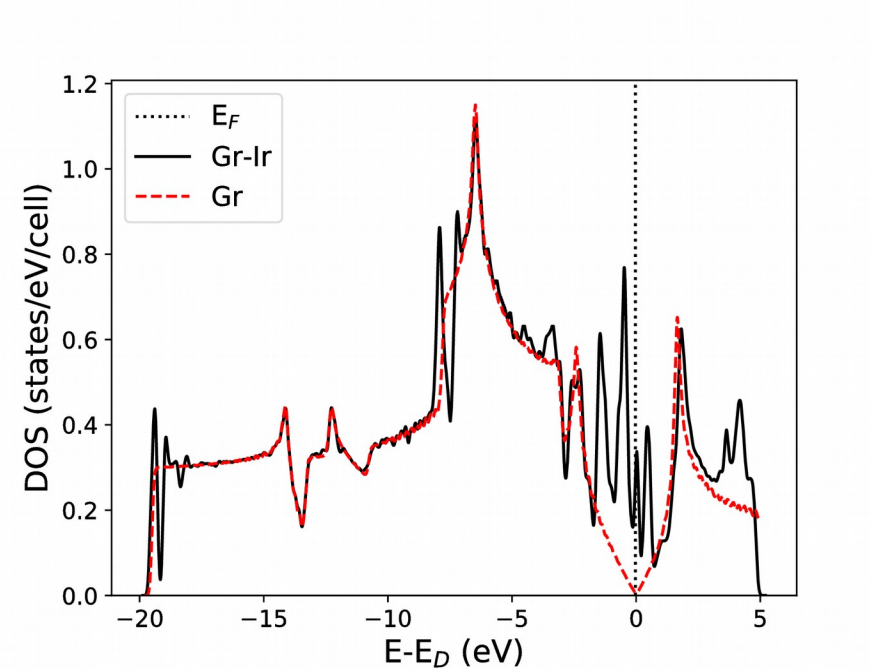

FIG. 3: The comparison between the calculated DOS for pristine graphene and for the single Ir adatom on graphene, in a 4x4 supercell. The DOS for the supercell is averaged over the number of primitive cells. The Fermi energy is identified by the dotted vertical line.

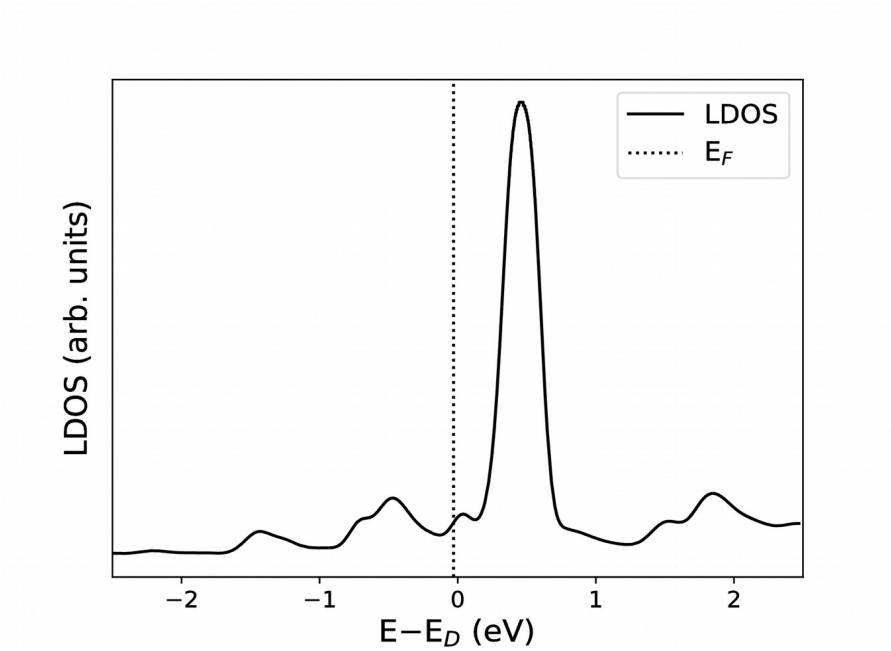

FIG. 4: The calculated LDOS for the single Ir adatom on graphene, measured 4 Å from the Ir atom. The Fermi energy is identified by the vertical dotted line.

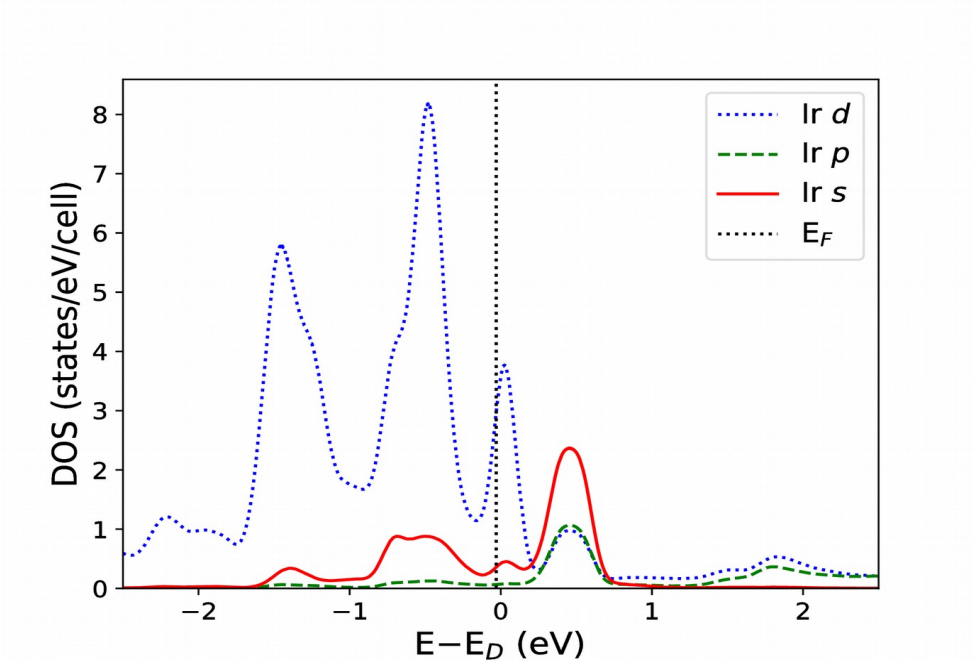

FIG. 5: The calculated PDOS for the single Ir adatom on graphene, with the zero of energy as the estimated Dirac point energy.

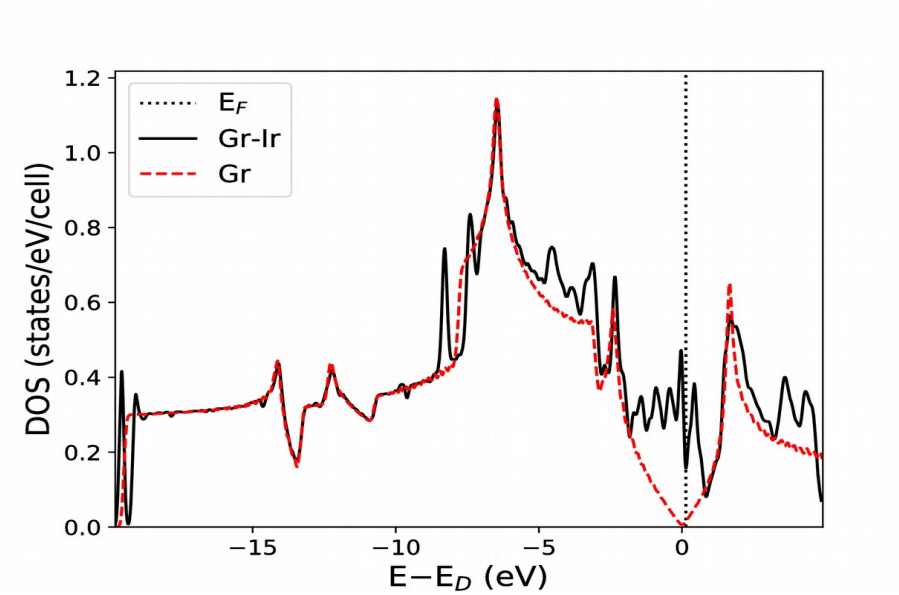

FIG. 6: The comparison of the calculated DOS for a pristine sheet of graphene and an Ir dimer adsorbed on graphene, in a 5x5 supercell. The DOS for the supercell is averaged over the number of primitive cells. The Fermi energy of the system is identified by the vertical dotted line.

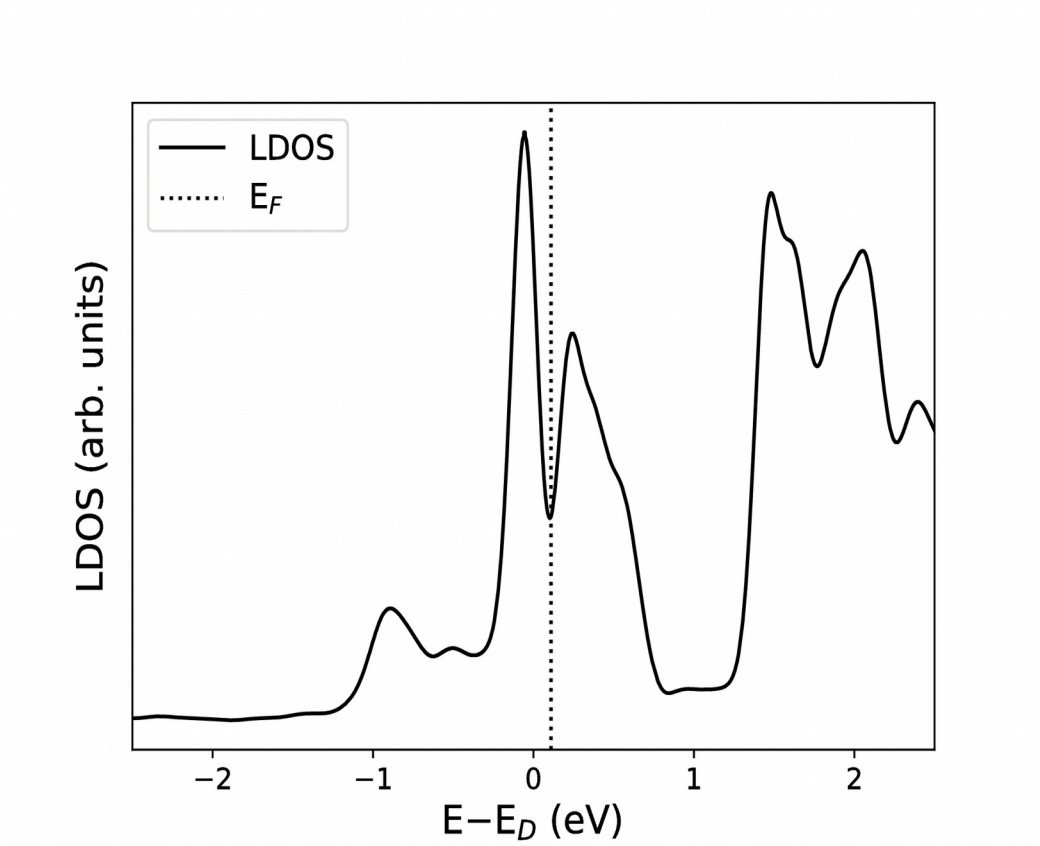

FIG. 7: The calculated LDOS for the Ir dimer on graphene, with the zero of energy as the estimated Dirac point energy. The states are 4 Å above the Ir atoms.

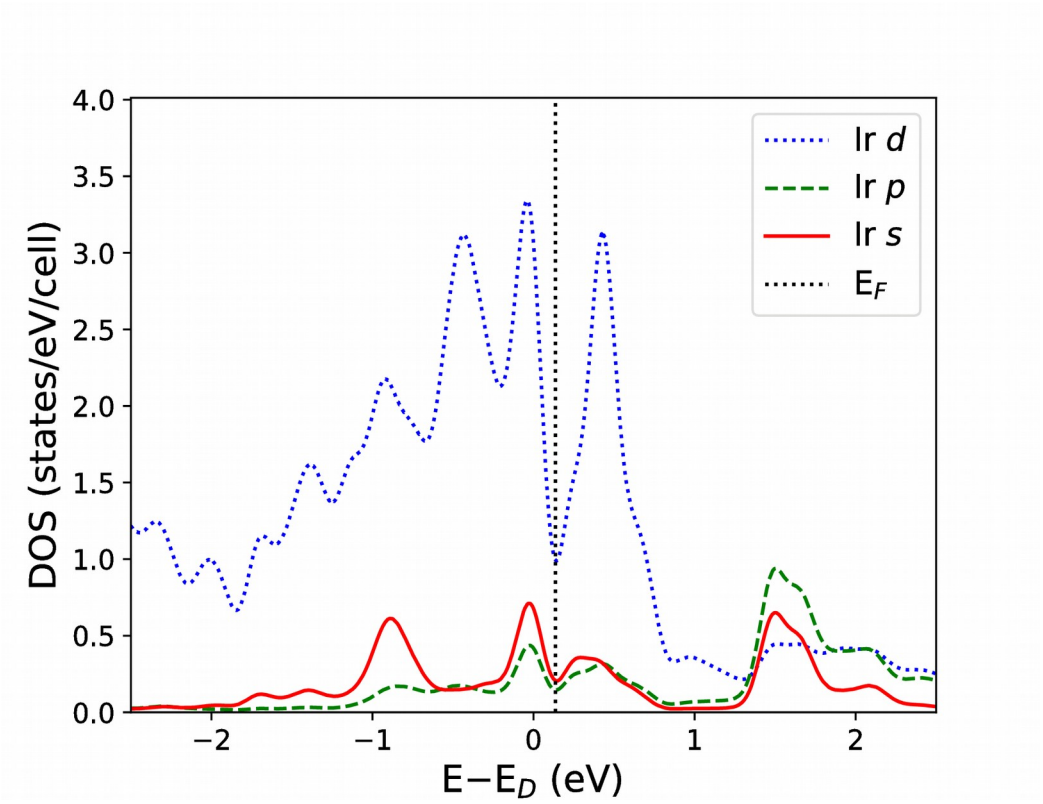

FIG. 8: The calculated PDOS for the Ir dimer on graphene, with the zero of energy as the estimated

Dirac point energy.

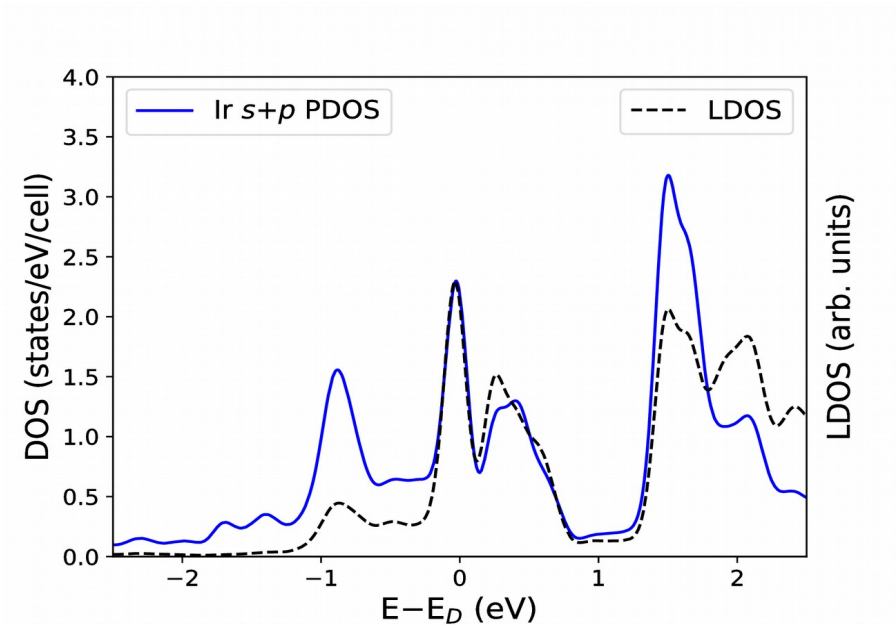

FIG. 9: The calculated PDOS from the sum of the Ir 6s and 6p orbitals, compared to the LDOS for the Ir dimer on graphene, with the zero of energy as the estimated Dirac point energy. The central peak in the LDOS is arbitrarily normalized to that of the PDOS for comparison.

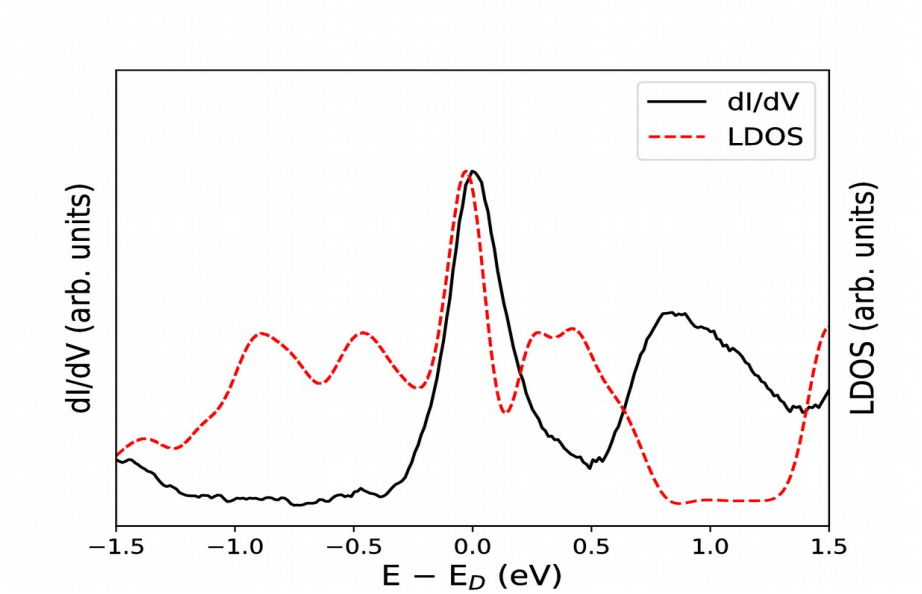

FIG. 10: Experimentally determined dI/dV for an Iridium cluster on graphene on a Pt(111) substrate, the solid black curve, compared with the calculated LDOS for the Ir dimer on graphene system, in dashed red. The energy is plotted relative to the estimated energy of the Dirac point.